# Relativistic approach for $e^{\pm}$ scattering from argon

Sultana N. Nahar

*Department of Astronomy, Ohio State University, Columbus, Ohio 43210*

J. M. Wadehra

*Department of Physics and Astronomy, Wayne State University, Detroit, Michigan 48202*

(Received 9 July 1990)

Differential and integrated elastic, integrated total cross sections as well as various polarization parameters—the spin polarization $P$ and the parameters $T$ and $U$ describing the change in the polarization vector during scattering—for the scattering of electrons and positrons from argon in the energy range of 3–300 eV are calculated using the relativistic Dirac equation. The real part of the projectile-target interaction is represented by a sum of model potentials. The phase shifts for large angular momenta $\hbar l$ are calculated using the Born approximation. The relativistic calculations for the differential and integrated elastic cross sections obtained using the pure real potential show almost no improvement over those obtained nonrelativistically for positron scattering from argon while similar calculations show some effects, except at low energies ( $\leq 5$ eV) where relativistic terms are sensitive to the form of potentials used, on the values of the differential cross sections for electron scattering from argon. The polarization parameter $P$ for electron scattering is found to be in good agreement with various calculated and measured values. A few different models of the absorption potential for the inelastic processes are used to calculate the integrated inelastic and the integrated total cross sections for positron and electron scattering from argon. It is noticed that even though the integrated elastic and the integrated total cross sections for the scattering of positrons and electrons calculated using some complex model potential agree well with the corresponding measured values, the differential cross section curves using the same model potentials can differ considerably from each other as well as from the experimental values.

## I. INTRODUCTION

Scattering of positrons and electrons (especially the electrons) by argon atoms has been an intensively studied problem for a long time (for references before 1987 see Ref. 1). In the present work, we investigate the same scattering problem using the *relativistic* approach, via the Dirac equation, which provides, in its standard formulation, the interaction effects of the projectile's spin. During the scattering of electrons and positrons (spin-$\frac{1}{2}$ particles) their magnetic moments interact with the magnetic field generated by the orbital motion of these particles with respect to the target atom, leading to the well-known spin-orbit interaction term. Hence, even though the incident beam of projectiles may be unpolarized, the spin-orbit interaction can orient the spins of the scattered particles in a preferred direction causing a net spin polarization. The study of spin polarization of the incident projectiles due to scattering provides more detailed information about the projectile-target interaction. The spin polarization of electrons during scattering by a central field was first investigated by Mott[2] using a relativistic treatment based on the theory of Dirac[3] The measurements of spin polarization parameters, however, are difficult and were not carried out for about one and a half decades after the prediction of Mott.[2] In general the spin-orbit interaction is a relatively weak interaction and does not have significant effect on the differential and in-

tegrated cross sections. Hence one could either introduce the spin-orbit interaction as a small perturbative term to the total projectile-target interaction in the Schrödinger equation or use the relativistic Dirac equation[3] which intrinsically includes this interaction along with other relativistic correction terms. In the present work, we start with the Dirac equation to describe the scattering system and calculate the differential and integrated elastic cross sections, momentum transfer cross sections, integrated total cross sections, and the polarization parameters, namely, the Sherman function $P$ as well as the parameters $T$ and $U$ relating the change in the polarization vector due to scattering in the impact energy range of 3–300 eV. In addition to representing the projectile-target interaction by a pure real model potential[1] for the elastic scattering of electrons or positrons from argon, we also use two model complex potentials to calculate the differential and the integrated cross sections. A few other models of the complex potential are used merely to observe the effects of these potentials on the features of the differential cross-section (DCS) curves.

## II. THEORY

### A. Setting up the radial Dirac equation

Consider a projectile of rest mass $m_0$ traveling with velocity **v** in a central field force $V(r)$ which can be either

real or complex. The total energy of the projectile is $E = m_0\gamma c^2 = E_i + m_0 c^2 = (p^2 c^2 + m_0^2 c^4)^{1/2}$ where $E_i$ is the kinetic energy of the projectile, $p = m_0\gamma v$ is its momentum, and $\gamma$ is given by $(1 - v^2/c^2)^{-1/2}$. The Dirac equation representing the system is

$$[c\boldsymbol{\alpha}\cdot\mathbf{p} + \beta m_0 c^2 + V(r) - E]\psi = 0 , \quad (1)$$

where the operators $\alpha$ and $\beta$ can be expressed by the usual $4\times4$ Dirac matrices[4] The spinor $\psi$ has four components, $\psi = (\psi_1, \psi_2, \psi_3, \psi_4)$ where $(\psi_1, \psi_2)$ are the "large" components and $(\psi_3, \psi_4)$ are the "small" components of $\psi$. For a central potential, a set of two homogeneous coupled equations satisfied by the radial parts of the large and the small components of $\psi$ can be obtained[5,6] from the Dirac equation (1) and these are often used as the starting point of scattering calculations. To obtain these coupled equations and the solution of Eq. (1), we follow a procedure similar to that described by Darwin.[5] Using the matrix representation[4] of the operators $\alpha$ and $\beta$ in Eq. (1) and defining $p_0 = (E - V)/c$, a set of four simultaneous equations satisfied by the four components of $\psi$ can be obtained[5] as

$$-\frac{i}{\hbar}(p_0 - m_0 c)\psi_1 + \left[\frac{\partial}{\partial x} - i\frac{\partial}{\partial y}\right]\psi_4 + \frac{\partial}{\partial z}\psi_3 = 0 , \quad (2a)$$

$$-\frac{i}{\hbar}(p_0 - m_0 c)\psi_2 + \left[\frac{\partial}{\partial x} + i\frac{\partial}{\partial y}\right]\psi_3 - \frac{\partial}{\partial z}\psi_4 = 0 , \quad (2b)$$

$$-\frac{i}{\hbar}(p_0 + m_0 c)\psi_3 + \left[\frac{\partial}{\partial x} - i\frac{\partial}{\partial y}\right]\psi_2 + \frac{\partial}{\partial z}\psi_1 = 0 , \quad (2c)$$

$$-\frac{i}{\hbar}(p_0 + m_0 c)\psi_4 + \left[\frac{\partial}{\partial x} + i\frac{\partial}{\partial y}\right]\psi_1 - \frac{\partial}{\partial z}\psi_2 = 0 . \quad (2d)$$

Since the potential $V(r)$ in Eqs. (2) is a function of $r$ only, each component $\psi_i$ ($i = 1,2,3,4$) of $\psi$ can be expressed as a product of a spherical harmonic $Y_{lm}$ and some radial function $R(r)$. Using the standard recursion relations[7] of spherical harmonics as well as Eqs. (A37)–(A39) of Ref. 4, all relevant derivatives of the product $R(r)Y_{lm}(\theta,\phi)$ can be evaluated easily. To begin with, if the angular part of $\psi_1$ is taken to be proportional to $Y_{lm}$, then one notes that the sum of the coefficients of various $Y_{lm}$'s arising from the first term as well as from the terms $(\partial/\partial x - i\partial/\partial y)\psi_4$ and $(\partial/\partial z)\psi_3$ of Eq. (2a) must vanish. This can be achieved by taking the same radial part for functions $\psi_3$ and $\psi_4$ and by making $\psi_3$ and $\psi_4$ proportional either to $Y_{l+1,m}$ and $Y_{l+1,m+1}$ or to $Y_{l-1,m}$ and $Y_{l-1,m+1}$, respectively. Similar arguments in Eq. (2c) suggest that $\psi_1$ and $\psi_2$ should contain the same radial function and have angular dependences of the form $Y_{lm}$ and $Y_{l,m+1}$. Therefore, one can choose

$$\psi_1 = a_1 G(r)Y_{lm}(\hat{\mathbf{r}}), \quad \psi_2 = a_2 G(r)Y_{lm,+1} ,$$

$$\psi_3 = -ia_3 F(r)Y_{l+1,m}, \quad \psi_4 = -ia_4 F(r)Y_{l+1,m+1} . \quad (3)$$

The factor $(-i)$ in $\psi_3$ and $\psi_4$ makes the radial function $F(r)$ real. The values of the coefficients $a$'s are adjusted such that all four simultaneous equations, Eqs. (2), are satisfied. Substituting the wave functions from Eqs. (3) and Eq. (2a) and using Eqs. (A37)–(A39) of Ref. 4, one gets

$$-\frac{i}{\hbar}(p_0 - m_0 c)a_1 GY_{lm} + ia_4\left[\left[\frac{(l-m+2)(l-m+1)}{(2l+3)(2l+5)}\right]^{1/2}Y_{l+2,m}\left[\frac{dF}{dr} - \frac{l+1}{r}F\right]\right.$$

$$\left. - \left[\frac{(l+m+2)}{(2l+1)}\frac{(l+m+1)}{(2l+3)}\right]^{1/2}Y_{lm}\left[\frac{dF}{dr} + \frac{l+2}{r}F\right]\right]$$

$$+ ia_3\left[-\left[\frac{(l+m+2)(l-m+2)}{(2l+3)(2l+5)}\right]^{1/2}Y_{l+2,m}\left[\frac{dF}{dr} - \frac{l+1}{r}F\right]\right.$$

$$\left. - \left[\frac{(l+m+1)(l-m+1)}{(2l+1)(2l+3)}\right]^{1/2}Y_{lm}\left[\frac{dF}{dr} + \frac{l+2}{r}F\right]\right] = 0 . \quad (4a)$$

It is seen that the terms proportional to $Y_{l+2,m}$ in this equation cancel for

$$a_3\sqrt{l+m+2} = a_4\sqrt{l-m+1} . \quad (4b)$$

Similarly substituting the wave functions of Eqs. (3) into Eq. (2c), we can write

$$-\frac{i}{\hbar}(p_0 + m_0 c)(-ia_3 FY_{l+1,m}) + a_2\left[-\left[\frac{(l-m+1)(l-m)}{(2l+1)(2l+3)}\right]^{1/2}Y_{l+1,m}\left[\frac{dG}{dr} - \frac{l}{r}G\right]\right.$$

$$\left. + \left[\frac{(l+m+1)}{(2l-1)}\frac{(l+m)}{(2l+1)}\right]^{1/2}Y_{l-1,m}\left[\frac{dG}{dr} + \frac{l+1}{r}G\right]\right]$$

$$+ a_1\left[\left[\frac{(l+m+1)(l-m+1)}{(2l+1)(2l+3)}\right]^{1/2}Y_{l+1,m}\left[\frac{dG}{dr} - \frac{l}{r}G\right]\right.$$

$$\left. + \left[\frac{(l+m)(l-m)}{(2l-1)(2l+1)}\right]^{1/2}Y_{l-1,m}\left[\frac{dG}{dr} + \frac{l+1}{r}G\right]\right] = 0 . \quad (5a)$$

Again in this equation we see that the sum of the coefficients of $Y_{l-1,m}$ cancel for

$$a_2\sqrt{l+m+1}=-a_1\sqrt{l-m} \ . \qquad (5b)$$

From the two conditions, Eqs. (4b) and (5b), on the coefficients $a$'s, the spinor components can be written as (apart from an overall constant)

$$\psi_1=\sqrt{l+m+1}\,G_l Y_{lm}, \quad \psi_2=-\sqrt{l-m}\,G_l Y_{l,m+1} \ ,$$

$$\psi_3=-i\sqrt{l-m+1}\,F_l Y_{l+1,m} \ , \qquad (6)$$

$$\psi_4=-i\sqrt{l+m+2}\,F_l Y_{l+1,m+1} \ .$$

where $F$ and $G$, the radial parts of the small and the large components of $\psi$, have been subscripted with $l$. Using the spinor components of Eqs. (6), Eqs. (4a) and (5a) reduce to a set of two coupled equations satisfied by $G_l$ and $F_l$:

$$\frac{1}{\hbar}(p_0-m_0c)G_l+\left[\frac{2l+3}{2l+1}\right]^{1/2}\left[\frac{dF_l}{dr}+\frac{l+2}{r}F_l\right]=0 \ ,$$

$$(7)$$

$$-\frac{1}{\hbar}(p_0+m_0c)F_l+\left[\frac{2l+1}{2l+3}\right]^{1/2}\left[\frac{dG_l}{dr}-\frac{l}{r}G_l\right]=0 \ . \quad (8)$$

These two equations can now be combined[8] to obtain a single equation for the large component $G_l$ which is similar to the radial Schrödinger equation. We denote

$$\eta=(p_0+m_0c)/\hbar, \quad \delta=(p_0-m_0c)/\hbar \ . \qquad (9)$$

Then substitution of the value of $F_l$ from Eq. (8) into Eq. (7) gives for the large radial component $G_l$ of $\psi$,

$$G_l''+\left[\frac{2}{r}-\frac{\eta'}{\eta}\right]G_l'+\left[\eta\delta+\frac{l\eta'}{r\eta}-\frac{l(l+1)}{r^2}\right]G_l=0 \ .$$

$$(10)$$

The prime and the double prime represent the first- and the second-order derivatives, respectively, with respect to $r$. Note that

$$\eta\delta=K^2-(2EV-V^2)/(\hbar^2c^2)$$

with

$$K^2=(E^2-m_0^2c^4)/(\hbar^2c^2) \ . \qquad (11)$$

If we choose atomic units ($m_0=e=\hbar=1$, $1/c=\alpha$, where $\alpha$ is the fine-structure constant) then $\eta=c(1+\gamma-\alpha^2V)$ and in terms of $K^2$ we can write $\gamma=(1-v^2/c^2)^{-1/2}=(1+\alpha^2K^2)^{1/2}$. Substituting

$$G_l=\sqrt{\eta}\,g_l/r \ , \qquad (12)$$

Eq. (10) can be rewritten as

$$g_l''(r)+\left[K^2-\frac{l(l+1)}{r^2}-U_l^+(r)\right]g_l(r)=0 \ , \qquad (13)$$

where, using atomic units and $E=\gamma c^2=\gamma/\alpha^2$,

$$-U_l^+(r)=-2\gamma V+\alpha^2V^2-\frac{3}{4}\frac{\eta'^2}{\eta^2}+\frac{1}{2}\frac{\eta''}{\eta}+\frac{l+1}{r}\frac{\eta'}{\eta} \ .$$

$$(14)$$

On the other hand, if the forms $Y_{l-1,m}$ and $Y_{l-1,m+1}$ were chosen for $\psi_3$ and $\psi_4$ instead of $Y_{l+1,m}$ and $Y_{l+1,m+1}$, a different set of coupled equations satisfied by the radial parts of the large and the small components of $\psi$ would have been obtained following the above procedure. In this case if we choose

$$\psi_1=a_1G(r)Y_{lm}(\hat{r}), \quad \psi_2=a_2GY_{l,m+1} \ ,$$

$$(15)$$

$$\psi_3=-ia_3F(r)Y_{l-1,m}, \quad \psi_4=-ia_4FY_{l-1,m+1} \ ,$$

and substitute these in Eqs. (2a) and (2c), it can be seen that the simultaneous equations are satisfied for

$$a_1\sqrt{l+m+1}=a_2\sqrt{l-m} \ ,$$

$$a_4\sqrt{l+m}=-a_3\sqrt{l-m-1} \ ,$$

so that Eqs. (15) can be written as

$$\psi_1=\sqrt{l-m}\,G_l Y_{lm}, \quad \psi_2=\sqrt{l+m+1}\,G_l Y_{l,m+1} \ ,$$

$$\psi_3=-i\sqrt{l+m}\,F_l Y_{l-1,m} \ , \qquad (16)$$

$$\psi_4=i\sqrt{l-m-1}\,F_l Y_{l-1,m+1} \ .$$

With these choices of spinor components the following coupled equations satisfied by the radial parts of the large and the small components ($G_l$ and $F_l$) are obtained from Eqs. (2):

$$\frac{1}{\hbar}(p_0-m_0c)G_l+\left[\frac{2l-1}{2l+1}\right]^{1/2}\left[\frac{dF_l}{dr}-\frac{l-1}{r}F_l\right]=0 \ ,$$

$$(17a)$$

$$-\frac{1}{\hbar}(p_0+m_0c)F_l+\left[\frac{2l+1}{2l-1}\right]^{1/2}\left[\frac{dG_l}{dr}+\frac{l+1}{r}G_l\right]=0 \ .$$

$$(17b)$$

Combining these two equations for the large radial component $G_l$ of $\psi$ and replacing $G_l$ for $g_l$ as in Eq. (12), we can get

$$g_l''+\left[K^2-\frac{l(l+1)}{r^2}-U_l^-(r)\right]g_l(r)=0 \ , \qquad (18)$$

where in atomic units

$$-U_l^-(r)=-2\gamma V+\alpha^2V^2-\frac{3}{4}\frac{\eta'^2}{\eta^2}+\frac{1}{2}\frac{\eta''}{\eta}-\frac{l}{r}\frac{\eta'}{\eta} \ . \quad (19)$$

Equations (13) and (18) can be combined as

$$g_l^{\pm''}+\left[K^2-\frac{l(l+1)}{r^2}-U_l^{\pm}(r)\right]g_l^{\pm}(r)=0 \ . \qquad (20)$$

We shall refer to Eq. (20) as the Schrödinger equivalent of the Dirac equation. The potentials $U_l^{\pm}$ are the effective Dirac potentials. It should be noted that the last terms of $U_l^{\pm}$ in Eq. (14) and in Eq. (19) correspond to the two, one due to spin up and the other due to spin down, eigenval-

ues of the well-known spin-orbit interaction,[9]

$$\frac{1}{4m_0^2c^2}\frac{1}{r}\frac{dV(r)}{dr}\boldsymbol{\sigma}\cdot\mathbf{L} . \tag{21}$$

To include the spin-orbit interaction in the *nonrelativistic* treatment of the Schrödinger equation the above term is added as a small perturbation energy to the total projectile-target interaction. In Eq. (21) above, $\sigma$ is related to spin **S** as $\sigma=2\mathbf{S}$ and the value of $\langle\boldsymbol{\sigma}\cdot\mathbf{L}\rangle$ equals $l$ for $j=l+\frac{1}{2}$ and equals $-(l+1)$ for $j=l-\frac{1}{2}$.

The proper asymptotic solution of Eq. (20) can be written as

$$g_l^{\pm}(K,r)\underset{r\to\infty}{\sim}Kr[j_l(Kr)-\tan\delta_l^{\pm}n_l(Kr)] , \tag{22}$$

where $j_l$ and $n_l$ are the spherical Bessel functions of the first and the second kind, respectively. The plus and the minus signs attached to the phase shifts $\delta_l^{\pm}$ correspond to incident particles with spin up and with spin down, respectively. The phase shifts $\delta_l^{\pm}$ can be obtained from the values of the radial wave function $g_l^{\pm}$ at two adjacent points $r$ and $r+h$ ($h\ll r$) at very large $r$ as

$$\tan\delta_l^{\pm}=-\frac{(r+h)g_l^{\pm}(r)j_l(K(r+h))-rg_l^{\pm}(r+h)j_l(Kr)}{rg_l^{\pm}(r+h)n_l(Kr)-(r+h)g_l^{\pm}(r)n_l(K(r+h))} . \tag{23}$$

In the present calculations the wave functions $g_l^{\pm}$ are obtained by numerical integration of Eq. (20) using the Numerov method and the spherical Bessel functions are evaluated as described in Ref. 1.

### B. Cross sections and spin polarization

The generalized scattering amplitude for the collision process is given by[10]

$$A=f(K,\theta)+g(K,\theta)\boldsymbol{\sigma}\cdot\hat{\mathbf{n}} \tag{24}$$

[the $r$-independent function $g(K,\theta)$ in the scattering amplitude above is not to be confused with the radial wave function $g_l^{\pm}$], where

$$f(K,\theta)=\frac{1}{2iK}\sum_{l=0}^{\infty}\{(l+1)[\exp(2i\delta_l^+)-1]$$
$$+l[\exp(2i\delta_l^-)-1]\}P_l(\cos\theta) \tag{25a}$$

and

$$g(K,\theta)=\frac{1}{2K}\sum_{l=0}^{\infty}[\exp(2i\delta_l^+)-\exp(2i\delta_l^-)]P_l^1(\cos\theta) , \tag{25b}$$

and $\hat{\mathbf{n}}$ is the unit vector perpendicular to the scattering plane. $P_l$ and $P_l^1$ are regular and associated Legendre polynomials, respectively. Since only the second term in the amplitude $A$ can induce change in spin states, $g(\theta)$ is often called the spin-flip amplitude. The differential cross section for the transition from an initial to a final state, for the case of an unpolarized incident beam, is given by

$$\frac{d\sigma}{d\Omega}=|f|^2+|g|^2 . \tag{26}$$

Since the spin-orbit interaction is a short-range interaction, the phase shifts for spin-up and spin-down cases are equal ($\delta_l^+=\delta_l^-$) for large angular momenta $l\hbar$. Hence for large $l$, $g(\theta)=0$ and the contribution to the scattering amplitude comes only from $f(\theta)$. If Born approximation is used for large $l>M$, $f(\theta)$ can be written as

$$f(K,\theta)=\frac{1}{2iK}\sum_{l=0}^{M}[(l+1)(S_l^+-1)+l(S_l^--1)]P_l$$
$$+f_B(K,\theta)-\frac{1}{2iK}\sum_{l=0}^{M}(2l+1)(S_{Bl}-1)P_l , \tag{27}$$

where $S_l^{\pm}=\exp(2i\delta_l^{\pm})$, $f_B$ is the Born amplitude, and $S_{Bl}=\exp(2i\delta_{Bl})$, $\delta_{Bl}$ being the Born phase shift. Evaluation of $f_B$ and $\delta_{Bl}$ for the case of real potential used in the present work is explained in Ref. 1. In the present work a large number of exact phase shifts were evaluated before using the Born approximation and hence the contribution due to Born approximation is found to be very small. The integrated elastic cross section for the unpolarized incident beam is obtained using

$$\sigma_{\text{el}}=2\pi\int_0^{\pi}(|f|^2+|g|^2)\sin\theta\,d\theta , \tag{28}$$

the integrated transport cross sections are given by

$$\sigma^{(n)}=2\pi\int_0^{\pi}(1-\cos^n\theta)(|f|^2+|g|^2)\sin\theta\,d\theta , \tag{29}$$

where $n=1,2,\ldots$; $n=1$ corresponds to the momentum transfer cross section. The integrated total cross section is given by

$$\sigma_{\text{tot}}=\frac{2\pi}{K^2}\sum_{l=0}^{\infty}\{(l+1)[1-\text{Re}(S_l^+)]$$
$$+l[1-\text{Re}(S_l^-)]\} , \tag{30}$$

and the integrated absorption cross section can be obtained as

$$\sigma_{\text{abs}}=\sigma_{\text{tot}}-\sigma_{\text{el}} . \tag{31}$$

The amount of polarization produced in the unpolarized incident beam due to the scattering is given by[10]

$$\mathbf{P}(\theta)=\frac{f^*g+fg^*}{|f|^2+|g|^2}\hat{\mathbf{n}}=P(\theta)\hat{\mathbf{n}} , \tag{32}$$

where $P(\theta)$ is often called the Sherman function. The other polarization parameters describing the rotation of polarization vector during the scattering process are

$$T(\theta)=\frac{|f|^2-|g|^2}{|f|^2+|g|^2}, \quad U(\theta)=i\frac{fg^*-gf^*}{|f|^2+|g|^2} . \tag{33}$$

The angle of rotation of the component of the polarization vector in the scattering plane is given by $\tan^{-1}(U/T)$. If $\delta_l^+=\delta_l^-$ ($g=0$), we see that $P=U=0$ while $T=1$. It should be noted that these three polarization parameters are interrelated through the condition $P^2+T^2+U^2=1$.

## C. Real and complex potentials

For the calculations in the present work, the real part $V_R(r)$ of the total potential $V(r)$ is the same as the nonrelativistic model potential of Ref. 1 where the projectile-target interaction was obtained by summing the static potential (repulsive) and the Buckingham-type model polarization potential (attractive) for positrons scattered from argon and by summing the static potential (attractive), the same polarization potential (attractive) and an exchange potential (attractive) for the electrons scattered from argon. The static potential is obtained using the nonrelativistic Slater-type orbitals of Roothan-Hartree-Fock wave functions given by Clementi and Roetti.[11] The same orbitals are used to obtain the electron density function in the electron exchange potential[12] and in the absorption potentials.[13,14] At low energies below the inelastic threshold the scattering is only elastic and $V(r)$ is represented purely by the real part $V_R(r)$. In the first part of the calculations we consider only the elastic scattering and represent $V(r)$ by $V_R(r)$ at all impact energies. In the latter part of the calculations $V(r)$ is represented by a complex potential and the scattering is considered total, that is, both the elastic and all the inelastic processes are included.

At projectile impact energies higher than the inelastic threshold energy (which is 8.96 eV for positronium formation during positron-argon scattering and 11.7 eV for the first excited state formation of the target during electron-argon scattering) other channels due to inelastic processes open up along with the elastic scattering channel. The cross section accounting for all these inelastic processes together is referred to as the absorption cross section and can be obtained by including an imaginary part $V_A$, known as the absorption potential, to the projectile-target interaction. This makes the complete projectile-target interaction complex as $V(r) = V_R(r) + iV_A(r)$. The absorption potential ($V_A$) describing all the inelastic processes during $e^{\pm}$ and rare-gas–atom scattering has been derived both empirically and nonempirically by several investigators (see the review article of Ref. 15 and the references cited in Ref. 13). The model absorption potential of Joachain and co-workers[15] is obtained using the Glauber eikonal approximation and is not analytical in nature. Among the most successful empirical model absorption potentials for $(e^-,\mathrm{Ar})$ scattering is that of Furness and McCarthy[16]

$$V_A = c\rho/T_l^2 \tag{34}$$

and $T_l = E - V_R$ is the local kinetic energy, $\rho$ is the charge density of the target and $c$ is an adjustable or empirical parameter. This model was modified later with good agreement with the experimental values of $(e^-,\mathrm{Ar})$ scattering by McCarthy et al.[17] as

$$V_A = c\rho_H/T_l^2 , \tag{35}$$

where $\rho_H$ is the density of the highest occupied orbital. It should be noted that the value of the empirical parameter $c$ depends on the impact energy and is different for electron and positron scattering for the same incident projectile energy since the inelastic processes for each case are different. similar to the above absorption potentials, Staszewska, Schwenke, and Truhlar[13] suggested a rather simple empirical form for $V_A$ as

$$V_A = c\rho . \tag{36}$$

In a more elaborate manner they[14] derived, by treating the rare-gas target as a free-electron gas, an expression for the absorption potential for electron scattering as

$$V_A = -\tfrac{1}{2}v\rho\bar{\sigma}_b , \tag{37}$$

where $v = [2(E - V_R)/m]^{1/2}$ is the local velocity of the projectile for $E - V_R \geq 0$ and $\bar{\sigma}_b$ is the average quasifree binary collision cross section obtained nonempirically using the free-electron gas model. The factor $\tfrac{1}{2}$ in Eq. (37) is introduced to account for the effect of exchange of the incident electron and the atomic electrons of the target during the scattering process. This potential can be adapted for positron scattering with the factor of one-half replaced by one since there is no exchange effect during positron-argon scattering. The most successful model of absorption potential of Truhlar and co-workers is the semiempirical quasifree binary collision model[13] in which two parameters $\alpha$ and $\beta$ are introduced in the expression for $\bar{\sigma}_b$ and these parameters are determined empirically. Both the nonempirical model [Eq. (37)] as well as the semiempirical model of Truhlar and co-workers[13,14] have been used in the present calculations for electrons and positrons scattered from argon.

## III. RESULTS AND DISCUSSIONS

### A. Elastic scattering processes
### using real potentials

We compare first the results of the present relativistic and the previous nonrelativistic calculations[1] of the elastic scattering of positrons and electrons from argon when the projectile-target interaction is represented by the purely real model potential $V_R$. Between the two projectiles, we first discuss the scattering of positrons and then of electrons. The contributions from the spin-orbit interaction term and the relativistic correction terms in the Dirac equation to the cross sections for the elastic scattering of positrons from argon are found to be very small and the values of the differential cross section (DCS) are almost the same (differing in the third or the fourth significant figures) as those of Ref. 1, which were obtained using the Schrödinger equation with no spin-orbit interaction. Hence the differential cross sections for the scattering of positrons by argon are not presented here in tables except for comparisons in figures. A possible reason for the small contributions from the aforementioned terms is the much weaker projectile-argon interaction (the short-range repulsive static potential and the long-range attractive polarization potential tend to cancel one another) in the case of positron scattering than for electron scattering. The present integrated elastic cross sections for positron scattering from argon are presented in Table I. These values are found to be close to those of

SULTANA N. NAHAR AND J. M. WADEHRA

TABLE I. Calculated and measured values of the integrated elastic and integrated total cross sections (in units of $a_0^2$) for *positrons* and *electrons* of various impact energies $E_i$ scattered from argon. The letters within parentheses next to the values of theoretical cross sections correspond to the type of potential used in the Dirac equation . RP corresponds to the use of purely real potential, CP and CP3 to the use of complex potentials that include the older version (Ref. 14) and version 3 (Ref. 13) of the absorption potential of Staszewska *et al.*

| $E_i$ | $\sigma_{el}$ (units of $a_0^2$) | | $\sigma_{tot}$ (units of $a_0^2$) | |
|---|---|---|---|---|
| (eV) | Theory | Experiment | Theory | Experiment |
| | | $(e^+,\mathrm{Ar})$ | | |
| 3 | 8.42 (RP) | 12.57,[a]8.32,[b]9.11[c] | | |
| 5 | 9.27 (RP) | 12.57,[a]9.68[c] | | |
| 10 | 11.77 (RP) | | 12.03 (CP) | 15.71,[a]14.76,[b] |
| | 11.76 (CP) | | 11.77 (CP3) | 14.33[c] |
| | 11.76 (CP3) | | | |
| 15 | 11.29 (RP) | | 17.40 (CP) | 20.89[d] |
| | 11.04 (CP) | | 11.76 (CP3) | |
| | 11.26 (CP3) | | | |
| 20 | 11.71 (RP) | | 23.96 (CP) | 22.84[d] |
| | 11.11 (CP) | | 12.78 (CP3) | |
| | 11.41 (CP3) | | | |
| 30 | 10.94 (RP) | | 30.37 (CP) | 25.73,[d]26.07[e] |
| | 10.62 (CP) | | 13.78 (CP8) | |
| | 10.49 (CP3) | | | |
| 40 | 10.40 (RP) | | 32.46 (CP) | 26.70,[f]29.85[e] |
| | 10.66 (CP) | | 14.58 (CP3) | |
| | 9.30 (CP3) | | | |
| 50 | 9.73 (RP) | | 32.69 (CP) | 26.2[d],28.21,[e] |
| | 10.64 (CP) | | 15.02 (CP3) | 25.92[f] |
| | 7.74 (CP3) | | | |
| 75 | 10.20 (RP) | | 30.75 (CP) | 24.16,[d]23.25[f] |
| | 10.43 (CP) | | 16.75 (CP3) | |
| | 7.37 (CP3) | | | |
| 100 | 9.56 (RP) | | 28.33 (CP) | 22.43,[d]15.39,[b]23.56,[e] |
| | 9.64 (CP) | | 16.09 (CP3) | 21.61[f] |
| | 6.91 (CP3) | | | |
| 150 | 8.61 (RP) | | 24.40 (CP) | 19.16,[d]19.48,[e]19.26[f] |
| | 8.14 (CP) | | 14.53 (CP3) | |
| | 6.08 (CP3) | | | |
| 200 | 7.91 (RP) | | 21.63 (CP) | 17.44,[d]15.24,[e] |
| | 7.08 (CP) | | 13.30 (CP3) | 16.65[f] |
| | 5.51 (CP3) | | | |
| 250 | 7.36 (RP) | | 19.57 (CP) | 13.51,[e]15.39[f] |
| | 6.30 (CP) | | 12.37 (CP3) | |
| | 5.16 (CP3) | | | |
| 300 | 6.90 (RP) | | 17.96 (CP) | 14.23,[d]12.88,[e] |
| | 5.72 (CP) | | 11.67 (CP3) | 13.82[f] |
| | 5.04 (CP3) | | | |
| | | $(e^-,\mathrm{Ar})$ | | |
| 3 | 13.32 (RP) | 19.65,[g]17.30,[h]20.15,[i] | | |
| | | 20.64[j] | | |
| 5 | 33.24 (RP) | 30.02,[g]30.87,[h]36.09,[i] | | |
| | | 36.76,[j]32.1[k] | | |
| 10 | 73.98 (RP) | 64.32,[g]67.54,[h]83.4,[i] | | |
| | | 71.4,[i]69.3,[j]73.47[k] | | |
| 15 | 85.98 (RP) | 75.04,[g]85.51[i] | 86.22 (CP) | 76.97,[d]85.3,[l]78.82[j] |
| | 85.78 (CP) | | 86.00 (CP3) | |
| | 85.97 (CP3) | | | |
| 20 | 73.14 (RP) | 68.4,[m]44.67,[g]71.31,[n] | 74.42 (CP) | 72.18,[h]61.89,[d]68.9,[l] |
| | 71.92 (CP) | 70.65[i] | 73.25 (CP3) | 68.75,[o]70.78,[j]67.97[k] |
| | 73.05 (CP3) | | | |
| 30 | 51.88 (RP) | 32.88,[g]47.21[n] | 55.19 (CP) | 46.18,[d]50.7,[l]47.66,[j] |

TABLE I. (Continued).

| E | (RP/CP/CP3) | | (CP/CP3) | |
|---|---|---|---|---|
| | 48.50 (CP)<br>51.55 (CP3) | | 52.23 (CP3) | 48.76,°51.89[k] |
| 40 | 40.38 (RP)<br>35.54 (CP)<br>39.81 (CP3) | 32.28[n] | 45.19 (CP)<br>40.95 (CP3) | 42.8,[l]41.94,°42.32,[j]<br>32.2[k] |
| 50 | 33.89 (RP)<br>28.09 (CP)<br>33.13 (CP3) | 25.6,[m]21.8,[g]26.48[n] | 39.54 (CP)<br>34.64 (CP3) | 35.5,[d]37.5,[l]36.65,°<br>36.19,[j]38.2[k] |
| 75 | 23.59 (RP)<br>17.90 (CP)<br>22.63 (CP3) | 14.29[g] | 30.57 (CP)<br>24.75 (CP3) | 29.9,[d]32.49° |
| 100 | 19.21 (RP)<br>12.04 (CP)<br>18.20 (CP3) | 17.1,[m]9.29,[g]18.66,[n]17.33,[p]<br>18.04,[q]16.51[r] | 25.22 (CP)<br>20.57 (CP3) | 27.39,[d]29.6,°28.58[k] |
| 150 | 14.88 (RP)<br>8.56 (CP)<br>13.90 (CP3) | 11.86,[n]13.33,[p]14.83,[q]13.21[r] | 20.22 (CP)<br>16.33 (CP3) | 22.65,[d]25.13,°23.77[k] |
| 200 | 12.66 (RP)<br>7.39 (CP)<br>11.76 (CP3) | 10.9,[m]9.81,[n]12.68,[q]11.09,[r]<br>11.51[s] | 17.56 (CP)<br>14.03 (CP3) | 20.04,[d]21.33,°20.84[k] |
| 250 | 11.25 (RP)<br>6.67 (CP)<br>10.45 (CP3) | | 15.70 (CP)<br>12.51 (CP3) | 18.92,°18.67[k] |
| 300 | 10.24 (RP)<br>6.13 (CP)<br>9.54 (CP3) | 7.82,[n]10.19,[q]8.81,[r]8.74[s] | 14.27 (CP)<br>11.40 (CP3) | 16.43,[d]17.47,°17.15[k] |

[a]Reference 18.
[b]Reference 19.
[c]Reference 20.
[d]Reference 33.
[e]Reference 49.
[f]Reference 50.
[g]Reference 24.
[h]Reference 31.
[i]Reference 32.
[j]Reference 36.

[k]Reference 37.
[l]Reference 34.
[m]Reference 22.
[n]Reference 25.
[o]Reference 35.
[p]Reference 26.
[q]Reference 27.
[r]Reference 28.
[s]Reference 29.

Ref. 1, up to almost four significant figures. The measured integrated elastic cross sections available at this time are only at energies below the positronium formation threshold and these compare favorably with the theoretical values of Table I. Relativistic calculations, using three different approximations, for positron scattering from argon have also been made by Bartschat, McEachran, and Stauffer.[21] Our present integrated elastic cross sections are larger than those obtained by Bartschat, McEachran, and Stauffer using both the polarized orbital method and the local polarization plus ten-state absorption potential but are smaller than those obtained using the ten-state optical potential. As in the cases of differential and integrated elastic cross sections, the values of the momentum transfer and higher transport cross sections for positron impact obtained in the present work are also about the same as those of Ref. 1, and hence they are not repeated here. The spin polarization $P$ and the other two spin-polarization parameters $T$ and $U$ for positron scattering from argon at various scattering angles have been calculated using only the real potential in the Dirac equation. Because of weak spin-orbit interaction for positrons, the values of the polarization $P$ and the parameter $U$ (which are not presented

here) are found to be very small (of the order of $10^{-5}$ and less) and the value of $T$ is almost 1 for all impact energies considered, indicating that measurement of these parameters for positrons incident on argon will be quite difficult.

For elastic scattering of electrons from argon, the contributions from the relativistic terms in the Dirac equation to the cross sections are comparatively more significant than those for positrons scattering from argon. The present relativistic DCS values at energies 20, 100, and 300 eV for elastic scattering of electrons from argon are compared with the theoretical nonrelativistic values of Ref. 1 and with various measured values[22-29] in Fig. 1. It is observed that for all electron impact energies considered, except 3 and 5 eV, the DCS curves for elastic scattering of electrons from argon obtained in the present work using the real potential are similar to those of Ref. 1 but show some differences at the minima and the maxima. Though the agreement is reasonable with the measured values of various investigators, it is not obvious whether the present relativistic results are much improved over the nonrelativistic results of Ref. 1. The disagreement between the relativistic and the nonrelativistic results at low impact energies, such as 3 and 5 eV,

can be explained by noting that the relativistic correction terms along with the spin-orbit interaction term become more sensitive to the form of potential used at lower energies. For example, the use of modified semiclassical exchange potential of Gianturco and Scialla[30] for electron scattering resulted in large cross sections at low energies
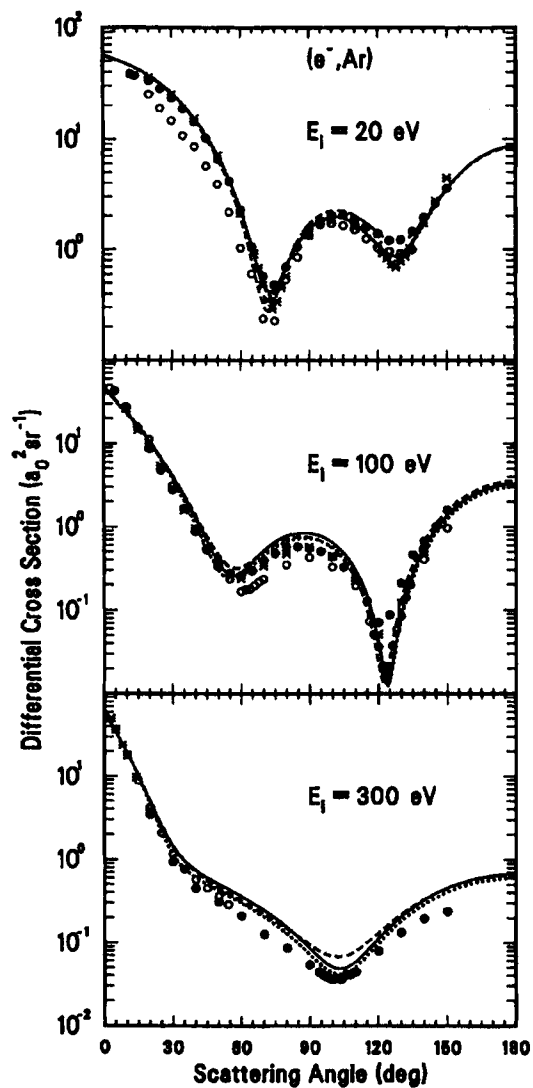
( $\leq 5$ eV) while at higher energies the cross sections stayed almost unchanged with respect to those obtained using the exchange potential of Riley and Truhlar[12] which has been used to obtain the values of all cross sections in the present work. The integrated relativistic cross sections for the elastic scattering of electrons from argon are compared with various measured values[22-28,31-37] in Table I and are shown in Fig. 2. Except at 3 eV, the calculated integrated cross sections agree well with the measured values. Elastic scattering of electrons from argon using relativistic approach has been investigated theoretically by Walker,[38] Fink and Yates,[39] Kemper et al.,[40] Sienkiewicz and Baylis,[41] and Bartschat, McEachran, and Stauffer.[21] The present cross sections for elastic scattering of electrons agree reasonably with those of Refs. 21 and 40. The differential and integrated cross sections of Sienkiewicz and Baylis[41] are closer, at lower energies, to the nonrelativistic values of Ref. 1 than to the present relativistic values while at energies higher than 10 eV their values agree well with the present values as well as with those of Ref. 1. The DCS values of Fink and Yates[39] differ significantly from the present results, and the cross sections calculated by Walker[38] cannot be compared directly since values are not tabulated in the reference. The present values of the integrated transport cross sections (for $n = 1-4$) are close to those of Ref. 1 except at electron impact energies $E_i \leq 5$ eV. The present calculat-



FIG. 1. The differential cross sections for the elastic scattering of electrons from argon. The solid curve corresponds to DCS values obtained in the present work using only the real potential in the Dirac equation, the dotted curve using the complex potential (V.3), and the dashed curve corresponds to the nonrelativistic values of Ref. 1. The experimental values are from Ref. 22 (solid circle), Ref. 24 (open circle), and Ref. 25 (asterisk) at 20 eV; Ref. 25 (open circle), Ref. 26 (solid circle), and Ref. 27 (asterisk) at 100 eV; Ref. 25 (solid circle), Ref. 28 (open circle), and Ref. 29 (asterisk) at 300 eV.
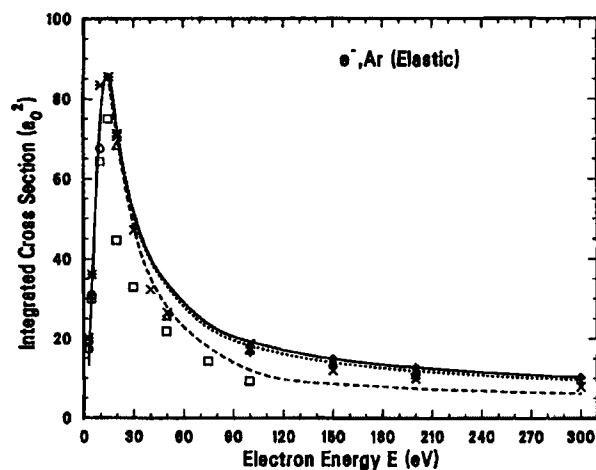


FIG. 2. The integrated cross sections for the elastic scattering of electrons from argon. The solid curve corresponds to the cross-section values obtained using the real potential in the Dirac equation and the dotted-dash curve (almost coinciding with the solid curve) corresponds to the nonrelativistic values from Ref. 1. The dotted curve and the dashed curve correspond to the use of complex potential in Dirac equation with absorption potentials represented by V.3 and the older version of Ref. 14, respectively. The experimental values are from Ref. 22 (open triangle), Ref. 24 (open squares), Ref. 25 (cross), Ref. 27 (diamond), Ref. 28 (plus), Ref. 31 (open circle), and Ref. 32 (asterisk).

ed momentum transfer cross sections ($n = 1$) are compared with the measured values[24,32] in Table II.

The values of the spin polarization $P$ for elastic scattering of *electrons* from argon at various impact energies cal-

culated in the present work using the *real* potential in the Dirac equation are shown and compared with a limited number of measurements in Figs. 3–5. Since the values of $P$ are measured more often than those of the parame-
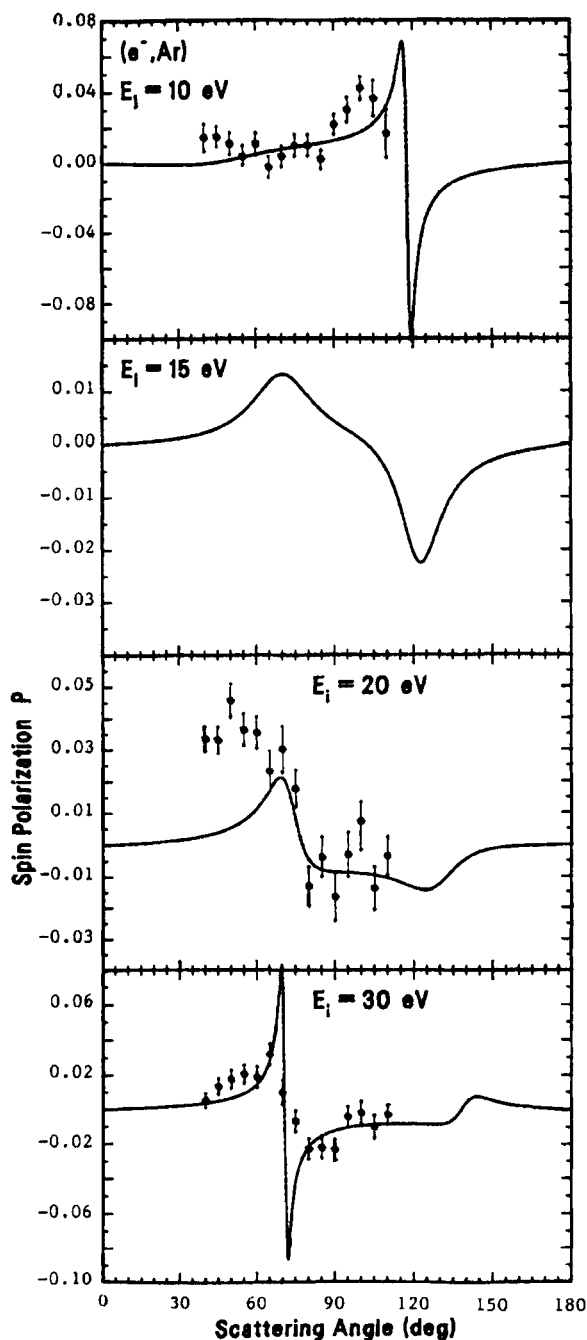


FIG. 3. The angular dependence of the spin polarization $P$ for elastic scattering of *electrons* from argon at various impact kinetic energies. The experimental values (solid circle) are read from the figures of Ref. 44 at 10, 20, and 30 eV.
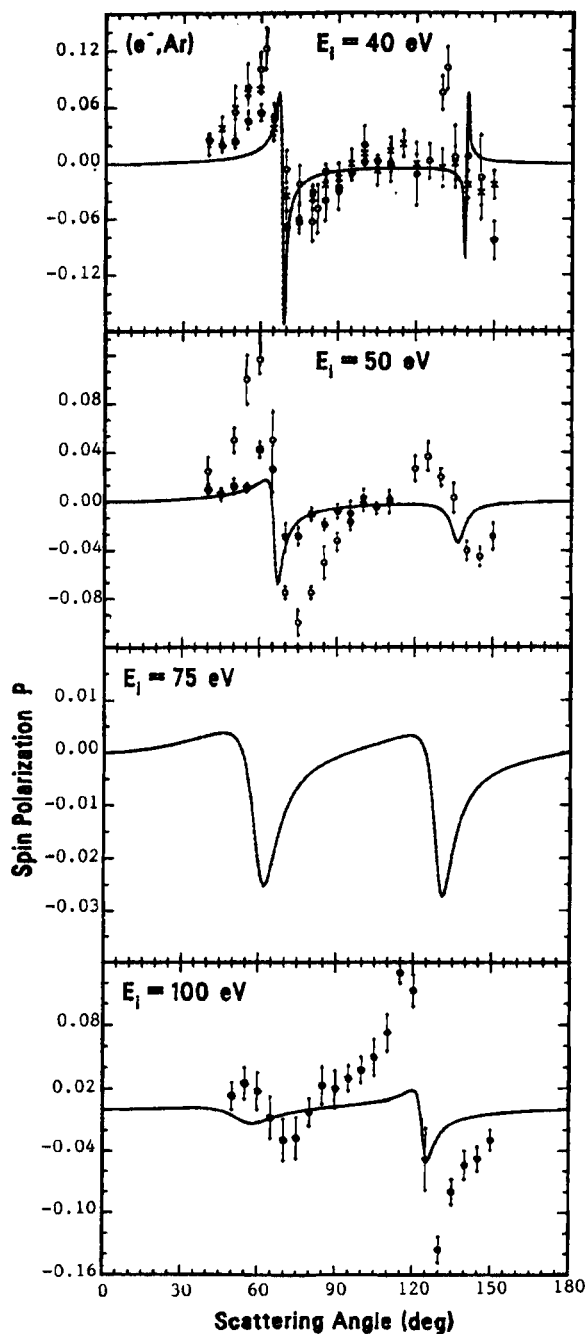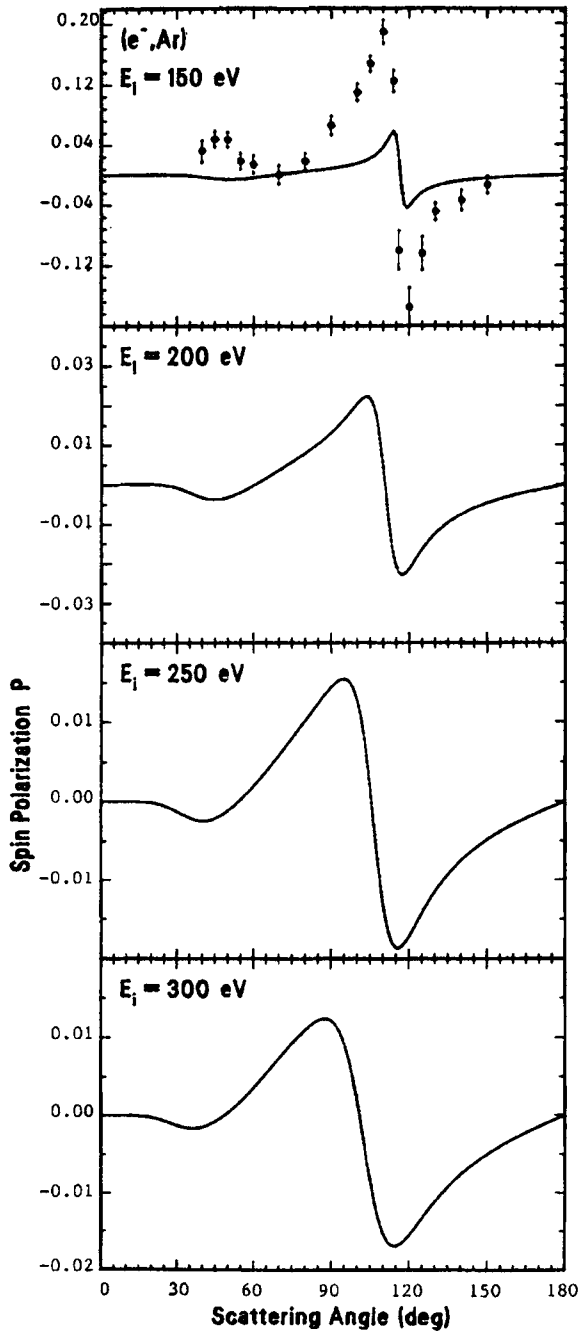
FIG. 4. The angular dependence of the spin polarization $P$ for elastic scattering of *electrons* from argon at various impact kinetic energies. The experimental values are read from the figures of Ref. 42 (open circles) at 40 eV, Ref. 44 (solid circle) at 40 and 50 eV, and Ref. 43 (cross) at 40 eV, (open circle) at 50 eV, (filled circle) at 100 eV.

ters $T$ and $U$ which are observed only in a "triple-scattering experiment," we present the numerical values of $P$ only for *electron* scattering from argon in Table III. Inversion of signs between the tabulated values of $P$ and

the curves of $P$ in Figs. 3–5 is irrelevant since directions of spin up and spin down are arbitrary. The spin polarization of *electrons* scattered elastically by argon at various angles has been measured by Mehr[42] at the impact energy of 40 eV, by Schackert[43] in the impact energy



FIG. 5. The angular dependence of the spin polarization $P$ for elastic scattering of *electrons* from argon at various impact kinetic energies. The experimental values are read from the figures of Ref. 38 (solid circle) at 150 eV.
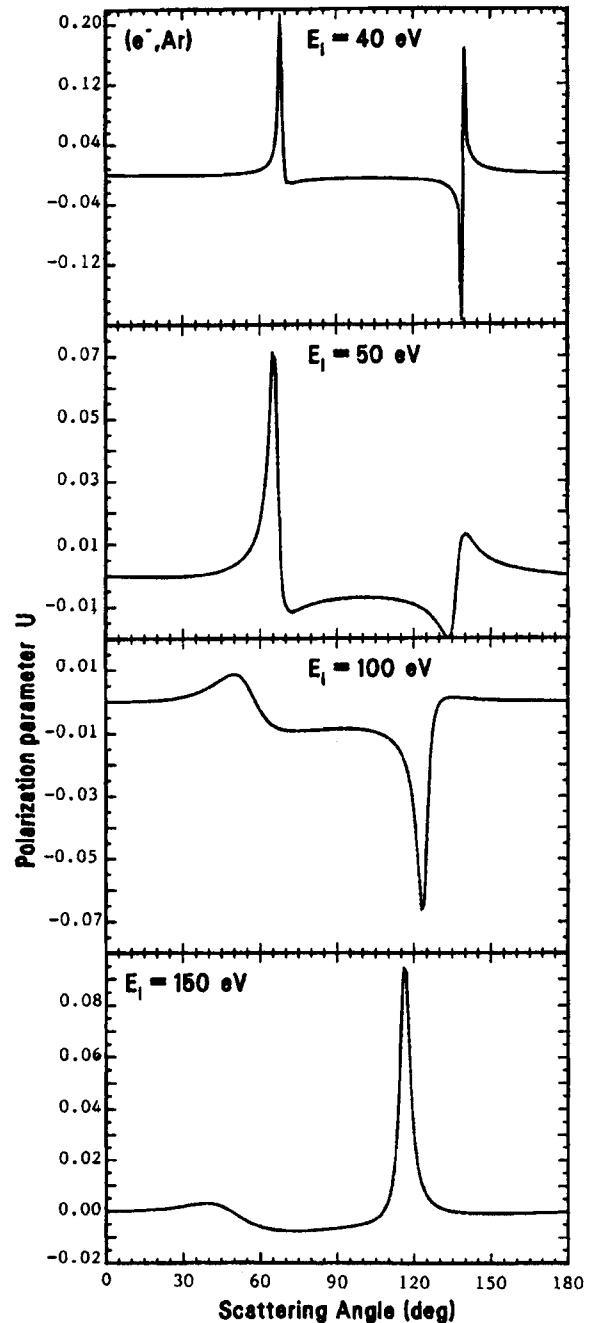
FIG. 6. The angular dependence of the spin polarization parameter $U$ for elastic scattering of *electrons* from argon at a few impact energies.

TABLE II. Calculated and measured values of integrated elastic momentum transfer cross sections, $\sigma^1$ (in units of $a_0^2$) for *electrons* scattered from argon at various electron impact energies $E_i$.

| $E_i$ (eV) | $\sigma^1$ (units of $a_0^2$) | | $E_i$ (eV) | $\sigma^1$ (units of $a_0^2$) | |
|---|---|---|---|---|---|
| | Calculated | Measured | | Calculated | Measured |
| 3 | 11.29 | 14.65,[a]16.72[b] | 50 | 15.03 | 8.58[a] |
| 5 | 30.27 | 22.87,[a]32.45[b] | 75 | 11.49 | 6.79[a] |
| 10 | 56.40 | 53.6,[a]67.65[b] | 100 | 9.50 | 5.72[a] |
| 15 | 47.85 | 53.6,[a]51.21[b] | 150 | 6.79 | |
| 20 | 32.29 | 23.58,[a]33.66[b] | 200 | 5.12 | |
| 30 | 20.31 | 13.22[a] | 250 | 4.03 | |
| 40 | 16.69 | | 300 | 3.27 | |

[a]Reference 24.
[b]Reference 34.

range of 40–150 eV, and by Beerlage, Qing, and Van der Wiel[44] in the energy range of 10–50 eV. For the purposes of comparing, the measured values of Refs. 42–44 were read from the figures presented in these papers and hence some reading errors in these values are expected. From Figs. 3–5, we see that the amount of polarization at various scattering angles agrees fairly well with those measured by Beerlage, Qing, and Van der Wiel[44] at 10, 30, 40, and 50 eV. At 20 eV, their measured values show higher polarization before the first theoretical peak while after the peak the measured polarization stays, on the average, close to the theoretical curve. Though there is some qualitative agreement in the angular distribution of the present calculated polarization with those of Refs. 42 and 43, their measured polarization is larger than the present values at all the energies considered. Theoretical investigations on the angular dependence of the polarization have been made by Walker,[38] Fink and Yates,[39]
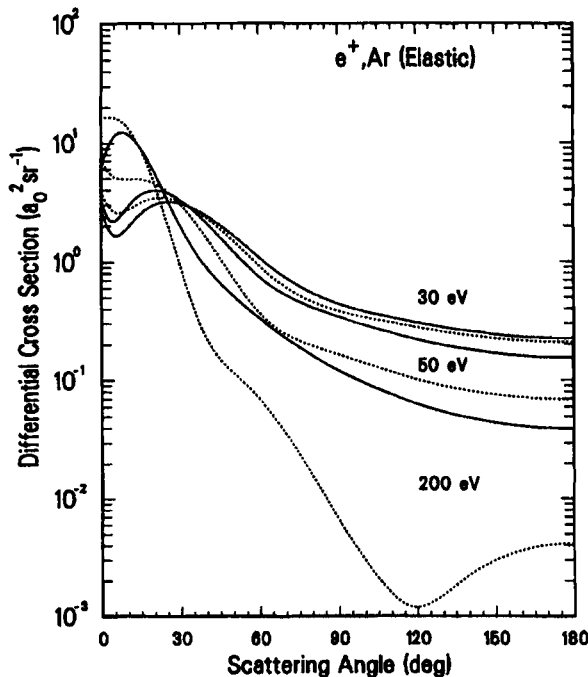


FIG. 7. Differential cross sections for elastic scattering from argon of positrons with impact energies of 30, 50, and 200 eV. For each energy the solid curve and the dotted curve represent DCS values obtained using the real potential and the version 3 of the complex potential, respectively.
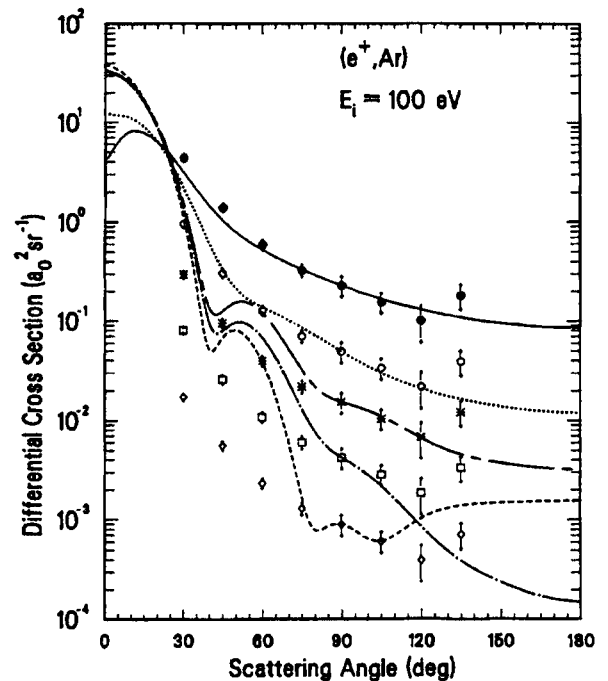


FIG. 8. The relativistic differential cross sections for the elastic scattering of *positrons* from argon at 100 eV using various model potentials. The solid curve represents the use of real potential and the rest of the curves correspond to the use of complex potential with various different model absorption potentials. The dotted curve corresponds to the model V.3, the dashed to the older version, dotted chain to Eq. (34), and the dashed chain to Eq. (36). A single set of experimental values taken from Ref. 47 are normalized to each theoretical curve at 90° (with different symbols) for comparison.

TABLE III. The values of the spin polarization $P$ of the *electron* beam elastically scattered by argon at various scattering angles $\theta$ obtained using the real potential in the Dirac equation at the impact kinetic energy range of $E_i = 3$–300 eV. The notation $a[b]$ means $a \times 10^b$.

| $\theta$ (deg) | Spin polarization $P$ at | | | | | | |
| | $E_i = 3$ eV | 5 eV | 10 eV | 15 eV | 20 eV | 30 eV | 40 eV |
|---|---|---|---|---|---|---|---|
| 0 | 0.0 | 0.0 | 0.0 | 0.0 | 0.0 | 0.0 | 0.0 |
| 5 | 0.147[−2] | 0.953[−3] | 0.209[−3] | −0.713[−4] | −0.153[−3] | −0.176[−3] | −0.161[−3] |
| 10 | 0.446[−2] | 0.228[−2] | 0.407[−3] | −0.182[−3] | −0.357[−3] | −0.425[−3] | −0.403[−3] |
| 15 | 0.111[−1] | 0.404[−2] | 0.583[−3] | −0.331[−3] | −0.610[−3] | −0.740[−3] | −0.724[−3] |
| 20 | 0.198[−1] | 0.605[−2] | 0.725[−3] | −0.522[−3] | −0.913[−3] | −0.112[−2] | −0.113[−2] |
| 25 | 0.180[−1] | 0.762[−2] | 0.806[−3] | −0.767[−3] | −0.128[−2] | −0.158[−2] | −0.162[−2] |
| 30 | 0.102[−1] | 0.776[−2] | 0.783[−3] | −0.109[−2] | −0.173[−2] | −0.214[−2] | −0.223[−2] |
| 35 | 0.522[−2] | 0.620[−2] | 0.584[−3] | −0.151[−2] | −0.230[−2] | −0.284[−2] | −0.299[−2] |
| 40 | 0.255[−2] | 0.386[−2] | 0.116[−3] | −0.210[−2] | −0.304[−2] | −0.373[−2] | −0.397[−2] |
| 45 | 0.925[−3] | 0.163[−2] | −0.717[−3] | −0.294[−2] | −0.406[−2] | −0.494[−2] | −0.529[−2] |
| 50 | −0.107[−3] | −0.136[−3] | −0.195[−2] | −0.418[−2] | −0.552[−2] | −0.667[−2] | −0.722[−2] |
| 55 | −0.817[−3] | −0.146[−2] | −0.350[−2] | −0.603[−2] | −0.775[−2] | −0.945[−2] | −0.104[−1] |
| 60 | −0.136[−2] | −0.246[−2] | −0.515[−2] | −0.865[−2] | −0.114[−1] | −0.146[−1] | −0.171[−1] |
| 65 | −0.179[−2] | −0.325[−2] | −0.668[−2] | −0.116[−1] | −0.172[−1] | −0.280[−1] | −0.403[−1] |
| 70 | −0.216[−2] | −0.391[−2] | −0.800[−2] | −0.132[−1] | −0.213[−1] | −0.773[−1] | 0.101 |
| 75 | −0.248[−2] | −0.451[−2] | −0.911[−2] | −0.119[−1] | −0.796[−2] | 0.438[−1] | 0.258[−1] |
| 80 | −0.279[−2] | −0.509[−2] | −0.101[−1] | −0.904[−2] | 0.456[−2] | 0.219[−1] | 0.148[−1] |
| 85 | −0.307[−2] | −0.570[−2] | −0.112[−1] | −0.634[−2] | 0.789[−2] | 0.151[−1] | 0.105[−1] |
| 90 | −0.334[−2] | −0.637[−2] | −0.125[−1] | −0.424[−2] | 0.855[−2] | 0.118[−1] | 0.827[−2] |
| 95 | −0.359[−2] | −0.715[−2] | −0.143[−1] | −0.254[−2] | 0.872[−2] | 0.995[−2] | 0.689[−2] |
| 100 | −0.377[−2] | −0.812[−2] | −0.171[−1] | −0.860[−3] | 0.898[−2] | 0.883[−2] | 0.600[−2] |
| 105 | −0.375[−2] | −0.930[−2] | −0.219[−1] | 0.133[−2] | 0.951[−2] | 0.815[−2] | 0.542[−2] |
| 110 | −0.315[−2] | −0.106[−1] | −0.320[−1] | 0.499[−2] | 0.105[−1] | 0.778[−2] | 0.506[−2] |
| 115 | −0.440[−3] | −0.106[−1] | −0.609[−1] | 0.117[−1] | 0.119[−1] | 0.768[−2] | 0.490[−2] |
| 120 | 0.120[−1] | 0.716[−2] | 0.898[−1] | 0.204[−1] | 0.136[−1] | 0.781[−2] | 0.499[−2] |
| 125 | 0.834[−1] | 0.674[−1] | 0.322[−1] | 0.215[−1] | 0.144[−1] | 0.814[−2] | 0.545[−2] |
| 130 | 0.978[−1] | 0.343[−1] | 0.176[−1] | 0.150[−1] | 0.122[−1] | 0.826[−2] | 0.677[−2] |
| 135 | 0.376[−1] | 0.184[−1] | 0.114[−1] | 0.959[−2] | 0.790[−2] | 0.565[−2] | 0.117[−1] |
| 140 | 0.189[−1] | 0.116[−1] | 0.806[−2] | 0.628[−2] | 0.434[−2] | −0.422[−2] | −0.732[−1] |
| 145 | 0.115[−1] | 0.800[−2] | 0.593[−2] | 0.430[−2] | 0.230[−2] | −0.750[−2] | −0.607[−2] |
| 150 | 0.765[−2] | 0.576[−2] | 0.445[−2] | 0.304[−2] | 0.124[−2] | −0.536[−2] | −0.256[−2] |
| 155 | 0.531[−2] | 0.422[−2] | 0.335[−2] | 0.219[−2] | 0.698[−3] | −0.352[−2] | −0.137[−2] |
| 160 | 0.373[−2] | 0.307[−2] | 0.248[−2] | 0.156[−2] | 0.403[−3] | −0.232[−2] | −0.806[−3] |
| 165 | 0.225[−2] | 0.215[−2] | 0.176[−2] | 0.108[−2] | 0.233[−3] | −0.150[−2] | −0.483[−3] |
| 170 | 0.160[−2] | 0.136[−2] | 0.112[−2] | 0.679[−3] | 0.129[−3] | −0.908[−3] | −0.276[−3] |
| 175 | 0.771[−3] | 0.663[−3] | 0.549[−3] | 0.329[−3] | 0.574[−4] | −0.428[−3] | −0.126[−3] |
| 180 | 0.0 | 0.0 | 0.0 | 0.0 | 0.0 | 0.0 | 0.0 |

| $\theta$ (deg) | Spin polarization $P$ at | | | | | | |
| | $E_i = 50$ eV | 75 eV | 100 eV | 150 eV | 200 eV | 250 eV | 300 eV |
|---|---|---|---|---|---|---|---|
| 0 | 0.0 | 0.0 | 0.0 | 0.0 | 0.0 | 0.0 | 0.0 |
| 5 | −0.141[−3] | −0.148[−3] | −0.122[−3] | −0.760[−4] | −0.416[−4] | −0.176[−4] | −0.150[−5] |
| 10 | −0.362[−3] | −0.357[−3] | −0.290[−3] | −0.172[−3] | −0.834[−4] | −0.220[−4] | 0.188[−4] |
| 15 | −0.666[−3] | −0.632[−3] | −0.508[−3] | −0.282[−3] | −0.107[−3] | 0.158[−4] | 0.963[−4] |
| 20 | −0.106[−2] | −0.985[−3] | −0.785[−3] | −0.384[−3] | −0.574[−4] | 0.169[−3] | 0.308[−3] |
| 25 | −0.157[−2] | −0.143[−2] | −0.111[−2] | −0.396[−3] | 0.202[−3] | 0.573[−3] | 0.743[−3] |
| 30 | −0.221[−2] | −0.198[−2] | −0.145[−2] | −0.112[−3] | 0.890[−3] | 0.130[−2] | 0.132[−2] |
| 35 | −0.300[−2] | −0.262[−2] | −0.163[−2] | 0.850[−3] | 0.208[−2] | 0.210[−2] | 0.168[−2] |
| 40 | −0.400[−2] | −0.329[−2] | −0.126[−2] | 0.279[−2] | 0.329[−2] | 0.245[−2] | 0.152[−2] |
| 45 | −0.531[−2] | −0.379[−2] | 0.599[−3] | 0.514[−2] | 0.378[−2] | 0.212[−2] | 0.838[−3] |
| 50 | −0.719[−2] | −0.329[−2] | 0.549[−2] | 0.638[−2] | 0.327[−2] | 0.117[−2] | −0.291[−3] |
| 55 | −0.102[−1] | 0.231[−2] | 0.121[−1] | 0.578[−2] | 0.200[−2] | −0.243[−3] | −0.177[−2] |
| 60 | −0.157[−1] | 0.215[−1] | 0.130[−1] | 0.395[−2] | 0.263[−3] | −0.196[−2] | −0.349[−2] |
| 65 | 0.741[−2] | 0.212[−1] | 0.914[−2] | 0.172[−2] | −0.168[−2] | −0.387[−2] | −0.536[−2] |
| 70 | 0.378[−1] | 0.118[−1] | 0.530[−2] | −0.464[−3] | −0.370[−2] | −0.588[−2] | −0.730[−2] |
| 75 | 0.166[−1] | 0.679[−2] | 0.249[−2] | −0.250[−2] | −0.576[−2] | −0.796[−2] | −0.920[−2] |
| 80 | 0.102[−1] | 0.399[−2] | 0.444[−3] | −0.443[−2] | −0.791[−2] | −0.101[−1] | −0.109[−1] |

TABLE III. (Continued).

| | | | | | | | |
|---|---|---|---|---|---|---|---|
| 85 | 0.718[−2] | 0.222[−2] | −0.116[−2] | −0.639[−2] | −0.103[−1] | −0.123[−1] | −0.122[−1] |
| 90 | 0.546[−2] | 0.971[−3] | −0.254[−2] | −0.856[−2] | −0.131[−1] | −0.144[−1] | −0.122[−1] |
| 95 | 0.434[−2] | −0.589[−5] | −0.387[−2] | −0.113[−1] | −0.165[−1] | −0.155[−1] | −0.931[−2] |
| 100 | 0.358[−2] | −0.842[−3] | −0.532[−2] | −0.151[−1] | −0.204[−1] | −0.127[−1] | −0.183[−2] |
| 105 | 0.304[−2] | −0.162[−2] | −0.710[−2] | −0.216[−1] | −0.219[−1] | −0.138[−2] | 0.844[−2] |
| 110 | 0.267[−2] | −0.237[−2] | −0.961[−2] | −0.358[−1] | −0.419[−2] | 0.133[−1] | 0.154[−1] |
| 115 | 0.249[−2] | −0.308[−2] | −0.137[−1] | −0.525[−1] | 0.210[−1] | 0.186[−1] | 0.169[−1] |
| 120 | 0.258[−2] | −0.320[−2] | −0.188[−1] | 0.418[−1] | 0.212[−1] | 0.172[−1] | 0.155[−1] |
| 125 | 0.338[−2] | 0.153[−2] | 0.468[−1] | 0.235[−1] | 0.164[−1] | 0.142[−1] | 0.133[−1] |
| 130 | 0.699[−2] | 0.254[−1] | 0.257[−1] | 0.150[−1] | 0.124[−1] | 0.115[−1] | 0.111[−1] |
| 135 | 0.273[−1] | 0.191[−1] | 0.137[−1] | 0.105[−1] | 0.960[−2] | 0.929[−2] | 0.919[−2] |
| 140 | 0.173[−1] | 0.105[−1] | 0.883[−2] | 0.779[−2] | 0.752[−2] | 0.750[−2] | 0.757[−2] |
| 145 | 0.558[−2] | 0.655[−2] | 0.620[−2] | 0.593[−2] | 0.593[−2] | 0.604[−2] | 0.619[−2] |
| 150 | 0.280[−2] | 0.447[−2] | 0.453[−2] | 0.456[−2] | 0.468[−2] | 0.483[−2] | 0.500[−2] |
| 155 | 0.171[−2] | 0.317[−2] | 0.336[−2] | 0.349[−2] | 0.364[−2] | 0.380[−2] | 0.397[−2] |
| 160 | 0.114[−2] | 0.226[−2] | 0.246[−2] | 0.262[−2] | 0.276[−2] | 0.291[−2] | 0.305[−2] |
| 165 | 0.756[−3] | 0.156[−2] | 0.173[−2] | 0.187[−2] | 0.199[−2] | 0.211[−2] | 0.222[−2] |
| 170 | 0.468[−3] | 0.987[−3] | 0.111[−2] | 0.121[−2] | 0.129[−2] | 0.137[−2] | 0.145[−2] |
| 175 | 0.225[−3] | 0.479[−3] | 0.540[−3] | 0.592]−3] | 0.635[−3] | 0.676[−3] | 0.715[−3] |
| 180 | 0.0 | 0.0 | 0.0 | 0.0 | 0.0 | 0.0 | 0.0 |

McCarthy et al.,[17] Kemper et al.,[40] and Sienkiewicz and Baylis.[45] The present results agree better with these other theoretical results, except Ref. 39, than with the measured values. Since no measured values of $U$ and $T$ are available at this time, the angular dependence of only $U$ at several impact energies is shown in Fig. 6. The present values of $U$ agree well with the calculated values of Ref. 45.

### B. Elastic and total scattering using complex potentials

Now we discuss the relativistic results of total, that is, elastic as well as inelastic, scattering of positrons and electrons from argon at impact energies above the inelastic threshold where the total projectile-target interaction is described by a complex optical potential. Both the nonempirical model [Eq. (37)] which will be referred to as the "older" version of the absorption potential and the semiempirical model[13] which, following the authors of Ref. 13, will be called version 3 (or simply V.3) of the absorption potential from now on, are used to calculate the elastic differential as well as the integrated elastic and integrated total cross sections for electrons and positrons scattered from argon. Again first we will discuss positron scattering from argon and then electron scattering. One incentive for using the complex potential, to include all inelastic processes during positron scattering from argon, was to observe the effect of the potential on the features of the differential cross section curves. The DCS values for elastic scattering of positrons from argon obtained using a complex potential with both models[13,14] of the absorption potential differ from each other at all energies considered. Below 40 eV the DCS curve obtained using the complex potential with absorption potential represented by V.3 stays close to that obtained using a real potential, shows a minimum after the forward peak, and then decreases slowly with larger scattering angles.

At higher energies the former starts to peak higher than the latter removing the minimum after the forward peak. These features can be seen in Fig. 7 where DCS curves using the real potential and using version 3 of the complex potential have been plotted for positron energies of 30, 50, and 200 eV. At 30 eV, both theoretical curves are seen to agree with the measured values of Floeder et al.[46] except in the rising part below 30°. But above 200 eV use of V.3 shows a minimum in the DCS values at large angle which is not observed experimentally.[47] On the other hand, the DCS curves obtained using the older version of
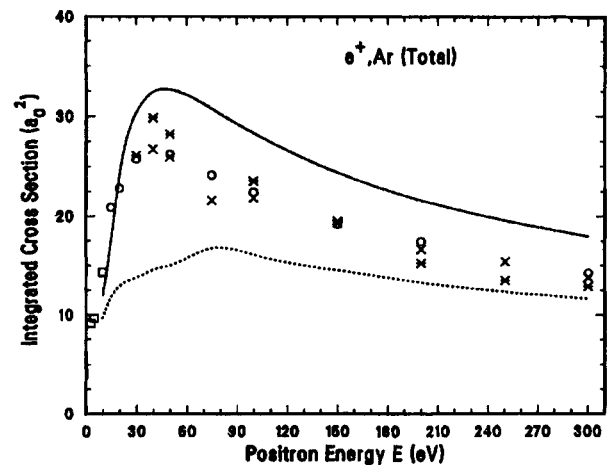


FIG. 9. The integrated total cross sections for positrons scattered from argon. The dotted curve corresponds to the use of V.3 while the solid curve to the older version of the model absorption potential. The experimental values are from Ref. 20 (open square), Ref.33 (open circle), Ref. 49 (asterisk), and Ref. 50 (cross).

the absorption potential show a shallow minimum near the forward direction below 30 eV which disappears forming a sharper peak in the forward direction and another minimum following it with higher impact energies. None of the DCS curves at various positron energies calculated using the older version of the absorption potential agree with the experimentally observed features of Refs. 46–48. To investigate the effect of the potential on the form of the DCS curves two other empirical model absorption potentials, Eqs. (34) and (36), were used to obtain the differential and the integrated elastic cross sections for 100-eV positrons scattered from argon. The empirical parameter $c$ in the absorption potential was varied to reproduce the observed integrated total cross sections. The elastic DCS curves for the scattering of positrons from argon at impact energy of 100 eV obtained using various absorption potentials are shown in Fig. 8. From this figure it can be seen that the DCS curve at 100 eV using the older version is very consistent, except at large angles, with those obtained using Eqs. (34) and (36) in values and features. From Table I we see that the values of the *integrated elastic* cross section obtained using the older model are much closer, below 200 eV, than those obtained using V.3 to the values obtained using only the real potential in the Dirac equation. The present integrated elastic cross sections obtained using both models[13,14] of the absorption potential lie between those obtained using two forms of complex potential by Bartschat, McEachran, and Stauffer.[21] The *integrated total* cross sections using the older nonempirical model seem to show, as in Fig. 9 and Table I, better agreement with the experimental values[33,49,50] than those obtained using V.3. It will be seen below that the older version generates better results for total integrated cross sections for electron scattering as well.

The DCS curves for elastic scattering of *electrons* from Ar, obtained using the V.3 absorption potential, agree nicely with the experimental values at all energies considered while those obtained using the older version[14] agree well up to 50 eV of the impact energies and then with higher impact energies start showing deeper and larger minima and lower peak at angles near backward scattering. The DCS curves for electron scattering obtained using both the real potential and the V.3 of the complex potential at energies 20, 100, and 300 eV are shown in Fig. 1 and it can be seen that the overall agreement with inclusion of V.3 is better than with those obtained using the real potential only. The calculated *integrated elastic* cross sections for *electrons* scattered from argon using the V.3 also agree better, as presented in Table I and shown in Fig. 2, than those using the older version at all energies. But for the *integrated total* cross section, use of the older version produces, as in the case of positron scattering also, values closer to the measured values as is seen in Table I and Fig. 10.

### C. Conclusions

In conclusion we summarize that elastic scattering of electrons and positrons from argon has been treated rela-
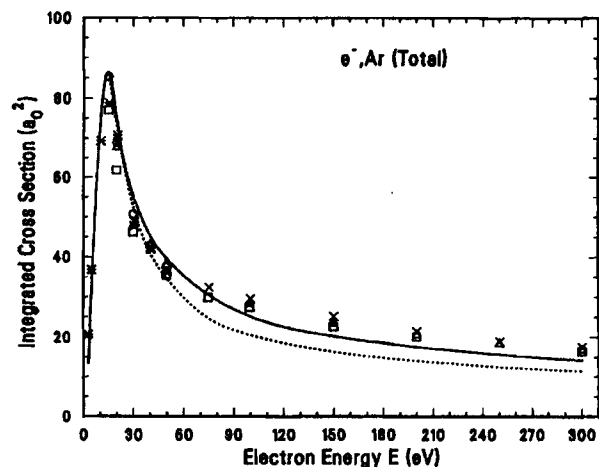


FIG. 10. The integrated total cross sections for *electrons* scattered from argon. The dotted curve corresponds to the use of V.3 while the solid curve to the older version. The experimental values are from Ref. 33 (open square), Ref. 34 (open circle), Ref. 35 (cross), Ref. 36 (asterisk), and Ref. 37 (open triangle).

tivistically by solving the Dirac equation numerically for the real model potential representing the projectile-target interaction. The calculated values of various cross sections (namely, differential and integrated elastic as well as momentum transfer) and the polarization parameters agree reasonably well with the available measured values except at low energies ( $\leq 5$ eV) for electron scattering. The dependence of the electron exchange potential on the radial distance, via the relativistic terms in the Dirac equation, becomes more important at low energies. In the case of total scattering, that is both the elastic and inelastic processes together, the calculated results and their comparison with the measured values depend on the model absorption potential used in the calculations. Though use of version 3 of the absorption potential[13] produces better results for elastic scattering of both the positrons and electrons from argon, the integrated total cross sections for both cases are much lower than the observed values. On the other hand, use of the "older" version of the absorption potential[14] produces better integrated total cross sections for both the positron and the electron scattering but poor results for the elastic cross sections. Use of two other empirical models of the absorption potential shows that even though good agreement can be obtained for the integrated cross sections by using various forms of the complex model potentials, the other features of the scattering processes such as the differential cross sections, polarization parameters, etc., may not show good agreement with the experimental values.

[1]Sultana N. Nahar and J. M. Wadehra, Phys. Rev. A **35**, 2051 (1987).

[2]N. F. Mott, Proc. R. Soc. London, Ser. A **124**, 425 (1929); **135**, 429 (1932).

[3]P. A. M. Dirac, Proc. R. Soc. London, Ser. A **117**, 610 (1928).

[4]See, for example, H. A. Bethe and E. E. Salpeter, *Quantum Mechanics of One- and Two-Electron Atoms* (Plenum/ Rosetta, New York, 1977).

[5]C. G. Darwin, Proc. R. Soc. London Ser. A **118**, 654 (1928).

[6]I. P. Grant, Adv. Phys. **19**, 747 (1970); J. P. Desclaux, Comput. Phys. Commun. **9**, 31 (1975).

[7]See, for example, G. Arfken, *Mathematical Methods for Physicists*, 2nd ed. (Academic, New York, 1970), p. 587.

[8]N. F. Mott and H. S. W. Massey, *The Theory of Atomic Collisions* (Oxford University, Oxford, 1987), p. 227.

[9]See, for example, R. M. Eisberg, *Fundamentals of Modern Physics* (Wiley, New York, 1961).

[10]See, for example, C. J. Joachain, *Quantum Collision Theory* (North-Holland, Amsterdam, 1983), Chap. 18.

[11]E. Clementi and C. Roetti, At. Data Nucl. Data Tables **14**, 177 (1974).

[12]M. E. Riley and D. G. Truhlar, J. Chem. Phys. **63**, 2182 (1975).

[13]G. Staszewska, D. W. Schwenke, and D. G. Truhlar, Phys. Rev. A **29**, 3078 (1984).

[14]G. Staszewska, D. W. Schwenke, D. Thirumalai, and D. G. Truhlar, Phys. Rev. A **28**, 2740 (1983).

[15]C. J. Joanchain, in *Proceedings of the 10th International Conference on the Physics of Electronic and Atomic Collisions*, edited by G. Watel (North-Holland, Amsterdam, 1978), p. 71.

[16]J. B. Furness and I. E. McCarthy, J. Phys. B **6**, 2280 (1973).

[17]I. E. McCarthy, C. J. Noble, B. A. Phillips, and A. D. Turnbull, Phys. Rev. A **15**, 2173 (1977).

[18]K. F. Canter, P. G. Coleman, T. C. Griffith, and G. R. Heyland, J. Phys. B **6**, L201 (1973); Appl. Phys. **3**, 249 (1974) (numerical values are quoted in Ref. 49).

[19]P. G. Coleman, T. C. Griffith, G. R. Heyland, and T. R. Twomey, Appl. Phys. **11**, 321 (1976); values of the integrated cross sections are read from the figure of this paper.

[20]W. E. Kauppila, T. S. Stein, and G. Jesion, Phys. Rev. Lett. **36**, 580 (1976).

[21]K. Bartschat, R. P. McEachran, and A. D. Stauffer, J. Phys. B **21**, 2789 (1988).

[22]R. D. DuBois and M. E. Rudd, J. Phys. B **9**, 2657 (1976) (data for integrated cross sections are quoted in Ref. 23).

[23]F. J. de Heer, R. H. J. Jansen, and W. van der Kaay, J. Phys. B **12**, 979 (1979).

[24]S. K. Srivastava, H. Tanaka, A. Chutjian, and S. Trajmar, Phys. Rev. A **23**, 2156 (1981).

[25]J. F. Williams and B. A. Willis, J. Phys. B **8**, 1670 (1975) (data for integrated cross sections are quoted in Ref. 23).

[26]L. Vusković and M. V. Kurepa, J. Phys. B **9**, 837 (1976) (data for integrated cross sections are quoted in Ref. 23).

[27]S. C. Gupta and J. A. Rees, J. Phys. B **8**, 1267 (1975); S. C. Gupta, Ph.D. thesis, University of Liverpool, 1975 (data for integrated cross sections are quoted in Ref. 23).

[28]R. H. J. Jansen, F. J. de Heer, H. J. Luyken, B. van Wingerden, and H. J. Blaauw, J. Phys. B **9**, 185 (1976) (data for integrated cross sections are quoted in Ref. 23).

[29]J. P. Bromberg, J. Chem. Phys. **61**, 963 (1974) (data for integrated cross sections are quoted in Ref. 23).

[30]F. A. Gianturco and S. Scialla, J. Phys. B **20**, 3171 (1987).

[31]J. Ferch, B. Granitza, C. Masche, and W. Raith, J. Phys. B **18**, 967 (1985).

[32]J. F. Williams, J. Phys. B **12**, 265 (1979) (Values for integrated elastic cross sections are quoted in Ref. 24).

[33]W. E. Kauppila, T. S. Stein, J. H. Smart, M. S. Dabaneh, Y. K. Ho, J. P. Downing, and V. Pol, Phys. Rev. A **24**, 725 (1981).

[34]K. Jost, P. G. F. Bisling, F. Eschen, M. Felsmann, and L. Walther, in *Abstracts of Contributed Papers, Thirteenth International Conference on the Physics of Electronic and Atomic Collisions, Berlin, 1983*, edited by J. Eichler, W. Fritsch, I. V. Hertel, N. Stolterfoht, and W. Willie (North-Holland, Amsterdam, 1983), p. 91 (data for integrated cross sections are quoted in Ref. 35).

[35]R. W. Wagenaar and F. J. de Heer, J. Phys. B **18**, 2021 (1985).

[36]M. Charlton, T. C. Griffith, G. R. Heyland, and T. R. Twomey, J. Phys. B **13**, L239 (1980).

[37]J. C. Nickel, K. Imre, D. F. Register, and S. Trajmar, J. Phys. B **18**, 125 (1985).

[38]D. W. Walker, Adv. Phys. **20**, 257 (1971).

[39]M. Fink and A. C. Yates, At. Data Nucl. Data Tables **1**, 386 (1970).

[40]F. Kemper, B. Awe, R. Rosicky, and R. Feder, J. Phys. B **16**, 1819 (1983).

[41]J. E. Sienkiewicz and W. E. Baylis, J. Phys. B **20**, 5145 (1987).

[42]J. Mehr, Z. Phys. **198**, 345 (1967).

[43]K. Schackert, Z. Phys. **213**, 316 (1968).

[44]M. J. M. Beerlage, Z. Qing, and M. J. Van der Wiel, J. Phys. B **14**, 4627 (1981).

[45]J. E. Sienkiewicz and W. E. Baylis, J. Phys. B **21**, 885 (1988).

[46]K. Floeder, P. Honer, W. Raith, A. Schwab, G. Sinapius, and G. Spicher, Phys. Rev. Lett. **60**, 2363 (1988).

[47]G. M. A. Hyder, M. S. Dababneh, Y.-F. Hsieh, W. E. Kauppila, C. K. Kwan, M. Mahdavi-Hezaveh, and T. S. Stein, Phys. Rev. Lett. **57**, 2252 (1986).

[48]S. J. Smith, G. M. A. Hyder, W. E. Kauppila, C. K. Kwan, and T. S. Stein, Phys. Rev. Lett. **64**, 1227 (1990).

[49]T. C. Griffith, G. R. Heyland, and T. R. Twomey, as reported by T. C. Griffith and G. R. Heyland, Phys. Rep. **39C**, 169 (1978).

[50]J.-S. Tsai, L. Lebow, and D. A. L. Paul, Can. J. Phys. **54**, 1741 (1976); values of the integrated cross sections are read from the figure of this paper.